A Modelling Study of Indoor Air Chemistry: The Surface Interactions of Ozone and Hydrogen Peroxide

Toby J. Carter [a], Dustin G. Poppendieck [b], David Shaw [a], Nicola Carslaw [a],*

[a] *Department of Environment and Geography, University of York, Wentworth Way, York, YO10 5NG, United Kingdom*
[b] *The University of Texas at Austin, Austin, TX 78712, United States of America*

HIGHLIGHTS

- Over 90% of indoor O_3 and H_2O_2 deposits onto indoor surfaces.
- Bedroom environments remove more O_3 and H_2O_2 than kitchens and offices.
- Deposition of O_3 increases indoor aldehyde concentrations.
- Surface reactivity should be accounted for when designing indoor air studies.

ARTICLE INFO

ABSTRACT

Indoor surfaces play a key role in indoor chemistry, including modification of indoor oxidant concentrations. This study utilises the INdoor CHEmical Model in Python (INCHEM-Py) to investigate the impact of surface transformations and their impact on indoor gas-phase chemistry. INCHEM-Py has been developed to simulate the surface deposition of ozone and hydrogen peroxide onto nine and six individual surfaces respectively in a typical bedroom, kitchen and office for normal indoor concentrations in the absence of household activities. The results show that 91 to 96% of these oxidants are deposited onto indoor surfaces under our simulated conditions. In the bedroom, 38 to 44% of indoor ozone and hydrogen peroxide is deposited onto soft fabric surfaces, with 41 to 54% of ozone deposition occurring on plastic surfaces in the kitchen and office. Total indoor concentrations of straight-chained aldehydes (C_1-C_{10}) ranged from $\approx$ 4 to 5 ppb, with nonanal having the highest individual concentration (1.7, 1.6 and 1.5 ppb in the bedroom, kitchen and office respectively), primarily as a result of emissions from plastics following ozone deposition. Aldehyde concentrations following hydrogen peroxide deposition were often less than 0.01 ppb. Understanding how reactions and deposition on different indoor surfaces impact indoor air chemistry will enable internal surface selection with a view to improving overall indoor air quality.

1. Introduction

The recent COVID-19 pandemic has highlighted the need for healthy indoor environments and the public is much more aware of the benefits of good indoor air quality. This is important as people spend approximately 90% of their time indoors (Klepeis et al., 2001), whether at home, at work, or commuting between the two.

Sources of indoor pollutants originate from a variety of household activities, including cooking (Kang et al., 2019) and cleaning (Carslaw et al., 2017; Carslaw and Shaw, 2022). Other notable sources include candle burning (Bekö et al., 2013) and emissions from indoor surfaces (Poppendieck et al., 2007b), which we will focus on in this study. These indoor pollutant sources release volatile organic compounds (VOCs), which can react with oxidants in the gas-phase to form

secondary pollutants, some of which are harmful to human health (Nørgaard et al., 2014).

The impact of internal surfaces on indoor gas-phase chemistry is an increasingly important area of focus (Ault et al., 2020). There are a wide range of surfaces indoors, such as carpets, wooden flooring, painted walls, and also the human surface (skin), which can act as both sinks and sources of indoor air pollutants (Fischer et al., 2013; Hodgson et al., 1993; Cheng et al., 2015; Katsoyiannis et al., 2008).

Indoor materials can emit pollutants either as primary emissions released directly from the surface, or as gas-phase transformation products that are formed following a surface interaction. Primary emissions released directly from indoor surfaces and building materials include a

---

Fig. 1. The chemical processes and transformations following deposition of oxidants on internal surfaces in the indoor environment.

wide array of chemical species, including carboxylic acids, aldehydes and alcohols (Chin et al., 2019; Ruiz-Jimenez et al., 2022). Emission rates of species emitted directly from surfaces are highest for new materials, but can continue to produce pollutants as they get older (Morrison and Nazaroff, 2002). In 30 Korean apartment buildings, approximately 60% of total indoor VOCs arose from flooring and paint materials (Shin and Jo, 2013).

Secondary pollutants can also be formed following gas-phase surface interactions, whereby a chemical reaction (often oxidation) with the surface instigates the release of secondary species. The emission rates of these secondary pollutants are important to quantify indoors, as they can be harmful to human health (Nazaroff and Weschler, 2004) and include aldehydes and ketones (Wang and Morrison, 2006; Cheng et al., 2015; Poppendieck et al., 2007b; Katsoyiannis et al., 2008; Salthammer, 2019; Destaillats et al., 2008), alkanes and alkenes (Hodgson et al., 1993), aromatics and esters (Xiong et al., 2019), and secondary organic aerosols (SOA) (Waring and Siegel, 2013). Wang and Morrison (2006) found that indoor surfaces continue to produce secondary pollutants over a long period of time, with 14-year old surfaces in a house still a source of secondary pollution.

Indoor surfaces can therefore modify indoor air composition. The composition of emitted species are surface dependent. Short and long-chain aldehydes are produced following ozone deposition onto soft fabrics (Cros et al., 2012; Lamble et al., 2011), whereas concrete surfaces emit short, straight-chain and aromatic aldehydes and ketones following ozone deposition (Poppendieck et al., 2007b). Although, it should be noted that these were the measured chemicals from the experimental studies. These surfaces likely emit other chemicals, but these studies were limited by the instrumentation and quantificational methods. Fig. 1 shows the surface interactions taking place in a standard home setting.

Skin can be an important contributor to indoor gas-phase chemistry, particularly in crowded spaces. Wang et al. (2022a) undertook a study of VOC emission rates from human skin, measuring a total VOC emission rate of 1150 µg hr^{-1} per person. This experiment was

performed on young adults with an average age of 25 years. Acetone and acetic acid had the largest emission rate from skin, contributing 16% and 19% of the total VOC emission respectively. The total VOC emission rate increased to 4450 µg hr^{-1} per person when ozone was present, suggesting that skin oxidation reactions were occurring and contributing to the VOC emissions from the skin surface (Wang et al., 2022a). Furthermore, Liu et al. (2021) discovered that products of ozone-skin lipid chemistry continued to contribute to measured VOC concentrations even in a home that had been empty for five days. This indicates that surfaces act as sources and reservoirs of VOCs indoors and can have a considerable effect on indoor chemistry.

Ozone can deposit onto a range of materials and surfaces indoors, where there are higher surface to volume ratios compared to outdoor environments. The respective rate of deposition of an oxidant indoors, such as ozone, depends on the type of surface and how that affects the transportation and uptake of the oxidant (Reiss et al., 1994). For example, fleecy surfaces, such as carpets, have a higher oxidant deposition velocity (Morrison and Nazaroff, 2000; Abbass et al., 2017) than smoother surfaces, such as wood or concrete (Schripp et al., 2012; Poppendieck et al., 2007a; Lin and Hsu, 2015). Deposition velocities of ozone onto indoor materials have been previously reviewed (Kruza et al., 2017; Shen and Gao, 2018). There is often a wide variation in these values, where the age, nature of the material surface, ozone concentrations and the measurement technique can all affect the deposition velocities that are determined through experiments (Lamble et al., 2011; Wang and Morrison, 2006).

Hydrogen peroxide (H_2O_2) can also play a role in indoor surface deposition (Zhou et al., 2020; Poppendieck et al., 2021). Often used as a cleaning agent, hydrogen peroxide can photolyse to form hydroxyl radicals (OH) (Kahan et al., 2012; Zhou et al., 2020), which drive indoor gas-phase chemistry. OH chemistry often dominates the gas-phase chemistry of indoor environments due to its high reactivity (Waring and Wells, 2015; Carslaw et al., 2017).

Poppendieck et al. (2021) determined the surface deposition velocities of hydrogen peroxide onto a range of common indoor surfaces,

including carpets and concrete and the consequent emissions of surface-formed species. Hydrogen peroxide deposition velocities which were higher (> 200 cm hr^{-1}), were found to be more sustained, compared to similar ozone deposition velocities, which were found to decay over time. However, over a 6-hr period of hydrogen peroxide exposure to indoor surfaces, less than 2 mg m^{-2} of secondary pollutants were emitted, lower than for ozone exposure onto similar surfaces, which emitted between 1 and 20 mg m^{-2} for wall coverings and flooring over 36 h (Poppendieck et al., 2021, 2007b). These hydrogen peroxide deposition velocities however were determined from extremely high concentrations that may have different mechanisms than for ambient concentrations.

There has, to date, been little focus on how surface deposition of hydrogen peroxide and subsequent surface interactions affect the indoor air chemistry. In fact, there is currently little experimental data evaluating the impact of surface deposition on indoor air chemistry other than ozone. Therefore, this study uses experimental data on surface deposition of ozone and hydrogen peroxide, as well as information relating to the extent and composition of indoor surfaces in three different indoor micro-environments, to improve an existing model for indoor air chemistry. We use the model to investigate the interaction of these two oxidants with internal surfaces and in so doing, gain a better understanding of the consequent impacts on indoor air chemistry.

2. Methods

2.1. The INCHEM-Py model

This study has been conducted using the INCHEM-Py model. INCHEM-Py is a detailed, chemical box model which predicts temporal concentrations of indoor air pollutant species (Shaw and Carslaw, 2021). INCHEM-Py uses the near-explicit Master Chemical Mechanism (MCM) v3.3.1 (http://mcm.york.ac.uk) as a mechanistic and kinetic dictionary of the degradation of 143 gas-phase VOCs and contains over 20,000 reactions (Jenkin et al., 1997) and approximately 6,000 species. Updates to the original MCM include degradation schemes for α- and β-pinene and non-aromatic VOCs (Saunders et al., 2003), aromatics (Bloss et al., 2005; Jenkin et al., 2003), β-caryophyllene (Jenkin et al., 2012) and isoprene (Jenkin et al., 2015).

The MCM does not consider lumping nor utilise surrogate species. Degradation mechanisms are initiated by the reaction of a VOC with ozone (Jenkin et al., 2020), OH (Jenkin et al., 2018), nitrate (NO$_3$) radicals (Jenkin et al., 2019) and photolysis where relevant. These initial processes produce hydroperoxy (HO$_2$), organic peroxy (RO$_2$), alkoxy (RO) and Criegee (R'R''COO) radicals as intermediate species, which themselves react in a further series of reactions until carbon dioxide (CO$_2$) and water (H$_2$O) are produced (Jenkin et al., 1997).

INCHEM-Py also includes terms for indoor photolysis (Wang et al., 2022b), indoor–outdoor air change, chlorine chemistry (Wong et al., 2017) and secondary organic aerosol (SOA) formation for three terpene species (Kruza et al., 2020; Carslaw et al., 2012). The operational working of the INCHEM-Py model is explained in Shaw and Carslaw (2021).

INCHEM-Py assumes a well mixed, spatial environment and predicts indoor gas-phase species' concentrations (C$_i$) over time by solving a series of coupled and stiff ordinary differential equations of the form:

$$\frac{dC_i}{dt} = \sum R_{ij} + (\lambda_r C_{i,out} - \lambda_r C_i) - v_{d_i}\left(\frac{A}{V}\right)C_i \tag{1}$$

where the first term on the right represents the sum of the rates of reaction involving species i with species j in the gas or particle phase. The second term is the indoor–outdoor change of species i, where λ_r is the air change rate (ACR) (s^{-1}), C$_{i,out}$ is the outdoor concentration of species i (molecule cm^{-3}) and C$_i$ is the indoor concentration of species i (molecule cm^{-3}). The final term relates to the irreversible surface deposition of species onto indoor materials, where, v_{d_i} represents the

deposition velocity of species i (cm s^{-1}), A represents the internal surface area (cm^2) and V is the total volume of the indoor environment (cm^3).

This study focuses on the final term in Eq. (1), and in particular, incorporates deposition of ozone and hydrogen peroxide onto internal surfaces and the resulting emissions of secondary pollutants from those surfaces. Whilst the ozone deposition and resulting emissions are an extension of the work by Kruza et al. (2017), the hydrogen peroxide treatment is a new addition to INCHEM-Py.

2.2. Development of the model

The first order loss rate of ozone ($F_{s_{O_3}}$) and hydrogen peroxide ($F_{s_{H_2O_2}}$) to a surface (in s^{-1}) can be calculated using Eq. (2) and Eq. (3) respectively (Kruza et al., 2017).

$$F_{s_{O_3}} = v_{d_{O_3}}\frac{A}{V} \tag{2}$$

$$F_{s_{H_2O_2}} = v_{d_{H_2O_2}}\frac{A}{V} \tag{3}$$

v_{dO_3} and $v_{dH_2O_2}$ represent the surface deposition velocities of ozone and hydrogen peroxide onto a material respectively (cm s^{-1}). Following an interaction at the surface, the emission rate, E_i (molecule cm^{-3} s^{-1}), of a secondary pollutant (species i), can be calculated using Eq. (4) and Eq. (5) for ozone and hydrogen peroxide deposition respectively (Morrison and Nazaroff, 2002; Kruza et al., 2017).

$$E_i = \frac{A v_{d_{O_3}} Y_i C_{O_3}}{V} \tag{4}$$

$$E_i = \frac{A v_{d_{H_2O_2}} Y_i C_{H_2O_2}}{V} \tag{5}$$

In Eqs. (4) and (5), Y_i is the production yield of species i emitted from a given surface (dimensionless) and will arise from a combination of reactions with, or displacement from, the surface. C_{O_3} and $C_{H_2O_2}$ are the concentrations of indoor ozone and hydrogen peroxide respectively (molecule cm^{-3}).

2.3. Oxidant deposition

For this work, we have considered ozone deposition onto nine surfaces and hydrogen peroxide deposition onto six surfaces, based on available literature. The range of deposition velocities of ozone (Sabersky et al., 1973; Lin and Hsu, 2015; Klenø et al., 2001; Grøntoft, 2002; Abbass et al., 2017; Gall et al., 2013; Tamás et al., 2006; Cros et al., 2012; Coleman et al., 2008; Ye et al., 2020; Lamble et al., 2011; Rim et al., 2016; Poppendieck et al., 2007a; Wang and Morrison, 2010, 2006; Nicolas et al., 2007; Morrison and Nazaroff, 2000; Fadeyi et al., 2013; Yao et al., 2020; Di et al., 2017; Rai et al., 2014; Fischer et al., 2013; Wisthaler and Weschler, 2010; Schripp et al., 2012; Mueller et al., 1973; Cox and Penkett, 1972; Grøntoft and Raychaudhuri, 2004; Simmons and Colbeck, 1990; Cano-Ruiz et al., 1993) and hydrogen peroxide (Poppendieck et al., 2021) are shown in Fig. 2 and Fig. 3 respectively. For the model simulations, the median deposition velocity value calculated was utilised.

2.4. Production yields of species from surfaces

The production yields of species emitted from a range of surfaces as a result of ozone and hydrogen peroxide deposition has been collated from a range of literature (Wang and Morrison, 2010; Weschler et al., 2007; Kruza and Carslaw, 2019; Cheng et al., 2015; Poppendieck et al., 2007b, 2021; Coleman et al., 2008), and are incorporated into the model (Table S1 and S2 in the Supporting Information).
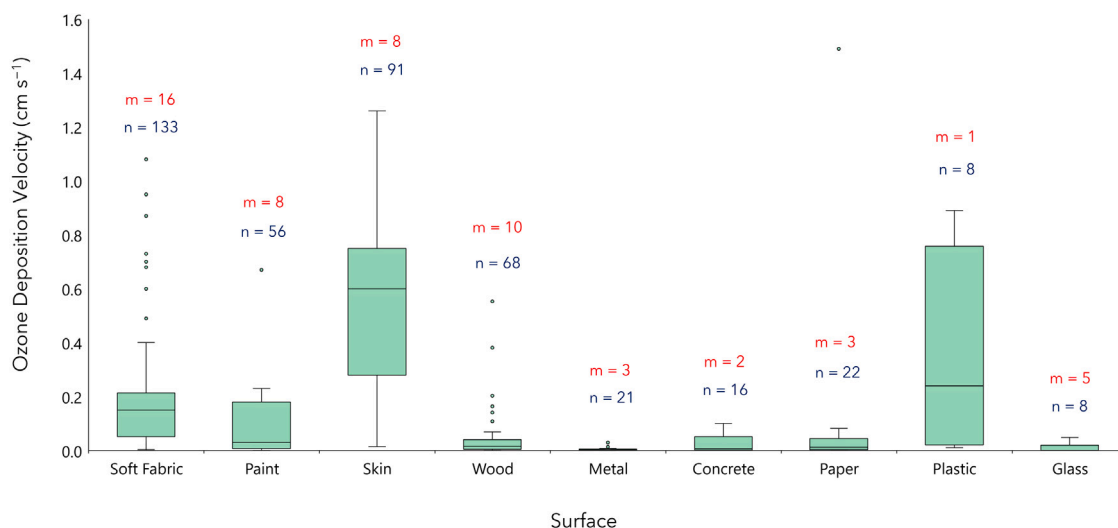
Fig. 2. The distribution of reported ozone deposition velocities onto a range of indoor surfaces, including the median, the upper (75% percentile) and lower (25% percentile) quartiles, the upper whisker (Q3 + 1.5*IQR) and the lower whisker (Q1 − 1.5*IQR) in cm s^{-1}. Values which fell outside the range of the upper and lower whiskers are also included in the plot as small circles. n denotes the total number of measurements per surface. m denotes the total number of studies consulted.
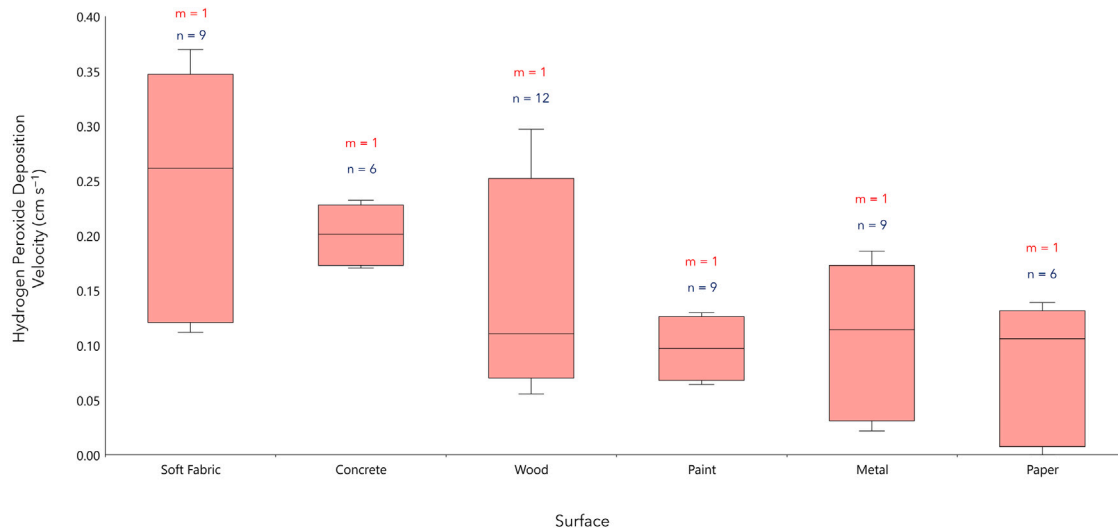

Fig. 3. The distribution of reported hydrogen peroxide deposition velocities onto a range of indoor surfaces, including the median, the upper (75% percentile) and lower (25% percentile) quartiles, the upper whisker (Q3 + 1.5*IQR) and the lower whisker (Q1 − 1.5*IQR) in cm s^{-1}. n denotes the total number of measurements per surface. m denotes the total number of studies consulted.

2.5. Indoor spatial representation

It is important to consider the surface area of a material in the indoor environment, to better understand how oxidant sorption onto materials and the transformations that subsequently occur impact indoor air quality (Manuja et al., 2019; Ye et al., 2020). Recent studies (Manuja et al., 2019; Hodgson et al., 2004; Morgan and Cruickshank, 2014) provide typical room sizes and surface area compositions. These studies provide the basis for predicting how replacing an indoor surface, for example a wooden floor, with an 'emission-free' or 'VOC friendly' alternative, will affect deposition, emissions and subsequently the impact on the overall indoor environment (Cheng et al., 2015).

Surfaces have been included in the INCHEM-Py model, and are categorised by material. For example, fleecy carpets and cushioned sofas are represented under the 'Soft Fabric' category, whereas wooden door frames and floors are assumed to be wooden surfaces. Most household items can then be considered in the model when analysing

indoor surface deposition. The total surface area of each specific surface is divided by the total volume of the indoor space to yield a surface-specific surface area-to-volume ratio.

Surface-specific area-to-volume ratios have been defined for a range of common indoor surfaces, using a comprehensive study which designated spatial representation in the indoor environment by Manuja et al. (2019). The study measured the total surface area of common indoor materials in bedrooms, kitchens and work offices. The surface areas of each material were then averaged for each room (Table S3, S4 and S5).

The total volumes of the bedroom, kitchen and office with their specific contents were 29, 25 and 35 m^3 respectively based on those calculated by Manuja et al. (2019). It was assumed that two adults would be present in the bedroom, one adult would be present in the kitchen and three adults present in the office. Adults are assumed to have $\approx$ 2 m^2 of skin surface (Fischer et al., 2013). Clothing is assumed to contribute to the 'skin' surface, as fabrics soiled with secreted skin oils and flakes have a similar ozone deposition velocity and retrospective secondary pollutant emission yields to bare skin Rai et al. (2014), Lakey et al. (2017), Kruza and Carslaw (2019).

2.6. Model parameterisation

The model was initialised to simulate a typical apartment located in suburban London. The temperature of the apartment was assumed to be 19.9 °C and the relative humidity 53.8%, based on the mean values from extensive monitoring of air quality in homes across the United Kingdom (Ministry of Housing, Communities & Local Government (UK Government), 2019).

Nazaroff (2021) undertook a comprehensive literature review of air change rates (ACR) in residential properties in Europe, North America and central Asia, and concluded that an appropriate median value of air change rates in homes is 0.5 hr^{-1}, with 95% of residential air change rates existing within a 0.125 and 2.0 hr^{-1} range. These findings were used to bound the ACR values in the model simulations.

Indoor photolysis rates are incorporated into the model and include the impact of indoor artificial light plus attenuated sunlight (Shaw and Carslaw, 2021; Wang et al., 2022b). For these simulations, incandescent lighting is used and the windows assumed to admit sunlight with a wavelength down to 308 nm ('Glass C' in Wang et al. (2022b)). The indoor lights were turned on at 07:00 GMT and switched off at 19:00 GMT. The date was assumed to be the 21st June and the latitude is set to that of central London, 51.5 °N.

The outdoor concentrations of key atmospheric species including OH, HO$_2$ and the methylperoxy radical (CH$_3$O$_2$), are defined in the model by diurnal profiles determined by the solar zenith angle (Carslaw, 2007). The outdoor concentrations of O$_3$, NO (nitric oxide) and NO$_2$ (nitrogen dioxide) were based on measurements in suburban London over the course of three months and follow a diurnal profile (Shaw and Carslaw, 2021; EEA, 2018). The average outdoor concentrations for these species are provided in Table S6.

The MCM is specifically designed to be an outdoor atmospheric degradation mechanism. Additional mechanisms for key indoor species not present in the MCM have been developed and incorporated in the INCHEM-Py model utilising experimental rate coefficients and oxidation pathways from literature. Additional degradation schemes in the INCHEM-Py model include; chlorine chemistry (Xue et al., 2015; Wong et al., 2017; Wang et al., 2020) and oxidation schemes for linalool (Carslaw et al., 2017), 2,5-dimethylbenzaldehyde (Clifford and Wenger, 2006; Jenkin et al., 1997), 2-nonenal (Gao et al., 2009; Gaona Colmán et al., 2017; Kerdouci et al., 2012), octanal, nonanal, decanal, Δ3-carene, camphene, and lactic acid (Shaw and Carslaw, 2021). The model also includes gas-to-particle partitioning for three monoterpenes; limonene, α-pinene and β-pinene (Carslaw et al., 2012). For the inclusion of humans in the model, breath emissions have also been added, using data from Kruza and Carslaw (2019), tailored according to how many adults are assumed to be present in each indoor space. These additional mechanisms have all been developed as ongoing improvements of INCHEM-Py (Shaw and Carslaw, 2021).

The model contains the concentrations of 110 outdoor VOCs and other atmospheric species which find their way indoors through ventilation (Shaw and Carslaw, 2021). The outdoor hydrogen peroxide concentration in the model is assumed to be 1.3 ppb, based on He et al. (2010). The outdoor VOC concentrations were sourced from experimental literature (Uchiyama et al., 2015; Baudic et al., 2016; Lü et al., 2006; Mentese and Bas, 2020; Bari and Kindzierski, 2018; Sturaro et al., 2010; Bari et al., 2016; Hakola et al., 2009; Brickus et al., 1998; Vichi et al., 2016; Liu et al., 2018; Gallego et al., 2016; Hellén et al., 2018; Dlugokencky, 2022; EEA, 2018) and are given in Table S7.

3. Results

3.1. The uptake of ozone and hydrogen peroxide on indoor surfaces

Kruza et al. (2017) found that 85% of the ozone present indoors was deposited onto indoor surfaces in their simulated apartment, conducted with an air change rate of 0.76 hr^{-1}. Similarly to this study, Kruza et al. (2017) also included surface specific deposition rates. This study has yielded comparable results, with 94, 91 and 94% of ozone deposited onto indoor surfaces in the bedroom, kitchen and office respectively. In addition, 96, 94 and 95% of indoor hydrogen peroxide is deposited onto indoor surfaces in the bedroom, kitchen and office respectively, with these model simulations using an air change rate of 0.5 hr^{-1}. These values reinforce the idea that indoor surfaces provide a key role in the removal of ozone and hydrogen peroxide in the indoor environment.

For an air change rate of 2.0 hr^{-1}, the total deposition of indoor ozone and hydrogen peroxide onto surfaces was 78 and 87% in the bedroom, 78 and 81% in the kitchen, and 86 and 84% in the office respectively. Under these higher air change rate conditions, more of the oxidant migrates to the outdoor environment before reacting with an indoor surface. Fig. 4 provides a breakdown of the percentage of the total deposition of ozone and hydrogen peroxide onto different indoor surfaces in the different study locations. The surface area percentage of each material in each room is also given in Fig. 4.

The importance of individual surfaces varies between rooms. For instance, soft fabric materials are responsible for 38% of the total ozone deposition in the bedroom, yet represents approximately 21% of the total surface area in the bedroom. Meanwhile, painted surfaces, which represents >45% of the bedroom surface area only contributes to 17% of the total ozone deposition. In the kitchen and the office, soft fabrics represents approximately 3% and 8% of the total surface area respectively. This leads to soft fabric surfaces being accountable for 7% and 11% of the total ozone deposition in these individual rooms. Plastic surfaces in the kitchen and the office are the most important ozone sink in these spaces, whilst metal, concrete, paper and glass surfaces are responsible for < 1% of ozone deposition, owing to small surface areas and low ozone deposition velocities. Despite a low overall surface area, deposition of ozone onto skin was the second biggest deposition sink in all three rooms, indicating the impact of occupants on ozone deposition indoors.

The rate of deposition of ozone onto indoor surfaces changes with room type and surface area of a material (Weschler, 2000). For example, the rate of deposition of ozone onto soft fabrics decreases by a factor of approximately 6 when moving from the bedroom to the kitchen, as there are fewer soft surfaces in the latter. For plastic surfaces, the rate of ozone deposition in an office is approximately 14 times more than the deposition rate in the bedroom. Painted surfaces have a more comparable impact in different rooms, where the total ozone deposition only fluctuates by approximately 10% between the office and the bedroom and kitchen.

Fig. 4 shows that indoor hydrogen peroxide deposition shows some similarities to ozone deposition. Soft fabrics are the most important material in the bedroom, accounting for 44% of the hydrogen peroxide deposition. However, unlike with ozone, hydrogen peroxide deposits predominantly onto painted surfaces in the kitchen (40%) and the office (32%). There is no data for hydrogen peroxide deposition onto plastic, glass and skin surfaces. Metallic surfaces have a larger proportion of hydrogen peroxide uptake than ozone in the kitchen and office, contributing to 15% of hydrogen peroxide uptake in both rooms. In absolute terms, the rates at which hydrogen peroxide deposits onto indoor surfaces are lower than for ozone, primarily due to the low indoor hydrogen peroxide concentration (averaged at 0.06 ppb over the three rooms). For hydrogen peroxide, the deposition rates are more closely aligned to the individual surface areas than ozone, given the deposition velocities vary over a smaller range than for ozone.

The average concentrations of key indoor species during the day (7 am–7 pm) are reported in Table 1, for scenarios with no deposition (baseline) and then also assuming empty or occupied (two people in the bedroom, one in the kitchen, three in the office) rooms. The occupied and unoccupied simulations include deposition for both ozone and hydrogen peroxide.

These modelled concentrations (including deposition) can be compared to experimental studies which measured indoor aldehyde species.
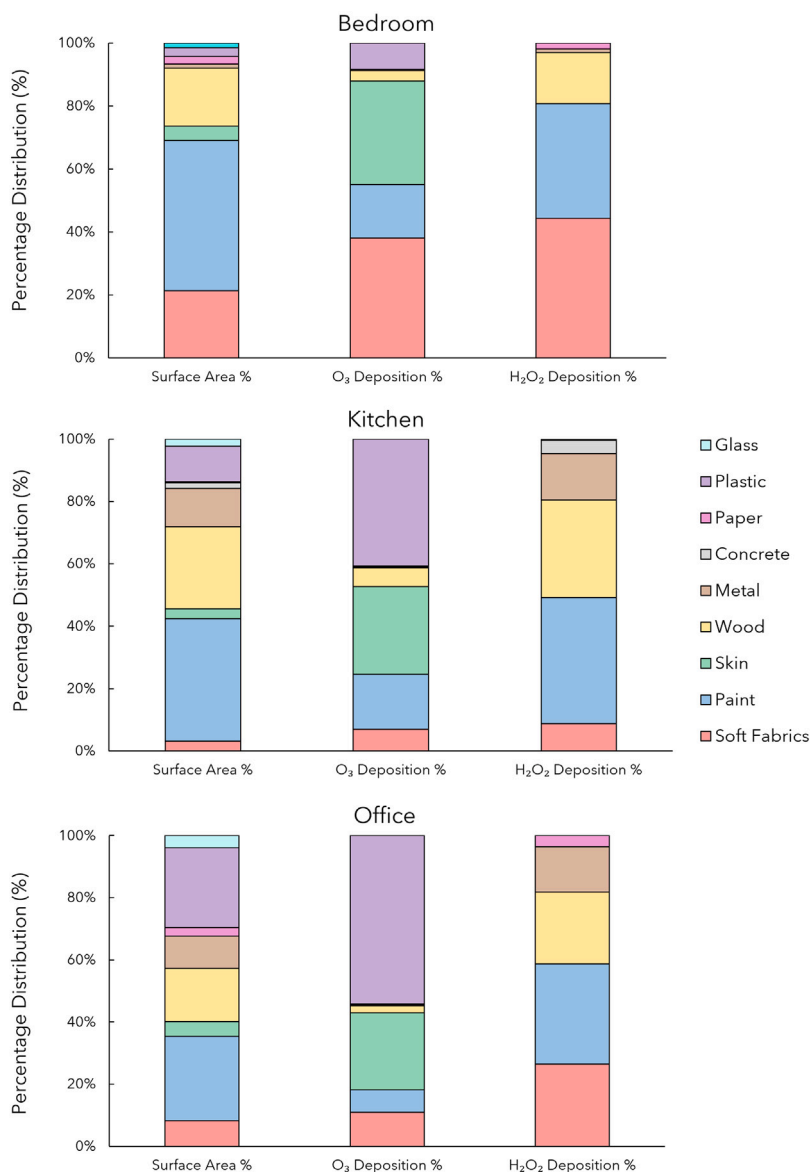
Fig. 4. The percentage distribution of ozone and hydrogen peroxide deposition by surface for the studied rooms. The total percentage surface area of each material in each room are also included.

Table 1

The average indoor concentration for a range of species in a bedroom, kitchen and office during the day, whilst the lights are on (7am to 7pm). The units for the concentration of OH is molecule cm^{-3}, the units for the concentration of HO_2 and RO_2 are ppt and the units for the rest of the species are given in ppb.

| Species	Baseline			Unoccupied			Occupied		
	Bedroom	Kitchen	Office	Bedroom	Kitchen	Office	Bedroom	Kitchen	Office
OH	1.1×10^6	1.2×10^6	9.9×10^5	8.9×10^5	9.7×10^5	8.6×10^5	7.4×10^5	9.0×10^5	6.1×10^5
HO_2	3.6	3.7	3.5	1.0	1.2	0.80	1.3	1.3	1.2
RO_2	5.8	5.7	5.9	1.6	1.9	1.2	1.7	1.9	1.5
O_3	26.6	27.0	26.1	2.5	3.5	1.5	1.8	2.7	1.2
NO	0.40	0.44	0.36	2.1	1.9	2.5	2.2	2.1	2.4
NO_2	0.76	0.88	0.65	0.59	0.70	0.45	0.55	0.66	0.44
Formaldehyde	0.38	0.45	0.31	0.62	0.79	0.47	0.63	0.77	0.53
Acetaldehyde	0.47	0.54	0.41	0.68	0.92	0.58	0.61	0.82	0.53
Propanal	0.13	0.15	0.12	0.25	0.33	0.18	0.21	0.28	0.16
Butanal	< 0.01	< 0.01	< 0.01	0.11	0.19	0.09	0.08	0.15	0.07
Pentanal	0.03	0.03	0.03	0.13	0.18	0.10	0.10	0.14	0.08
Hexanal	0.03	0.04	0.03	0.19	0.17	0.11	0.14	0.14	0.09
Heptanal	0.02	0.03	0.02	0.07	0.06	0.06	0.05	0.05	0.05
Octanal	0.08	0.08	0.08	0.24	0.21	0.22	0.20	0.18	0.20
Nonanal	0.47	0.46	0.48	2.0	1.7	1.6	1.8	1.6	1.5
Decanal	0.13	0.13	0.13	0.66	0.73	0.73	0.75	0.77	0.82
4-OPA	< 0.01	< 0.01	< 0.01	< 0.01	< 0.01	< 0.01	0.08	0.08	0.06
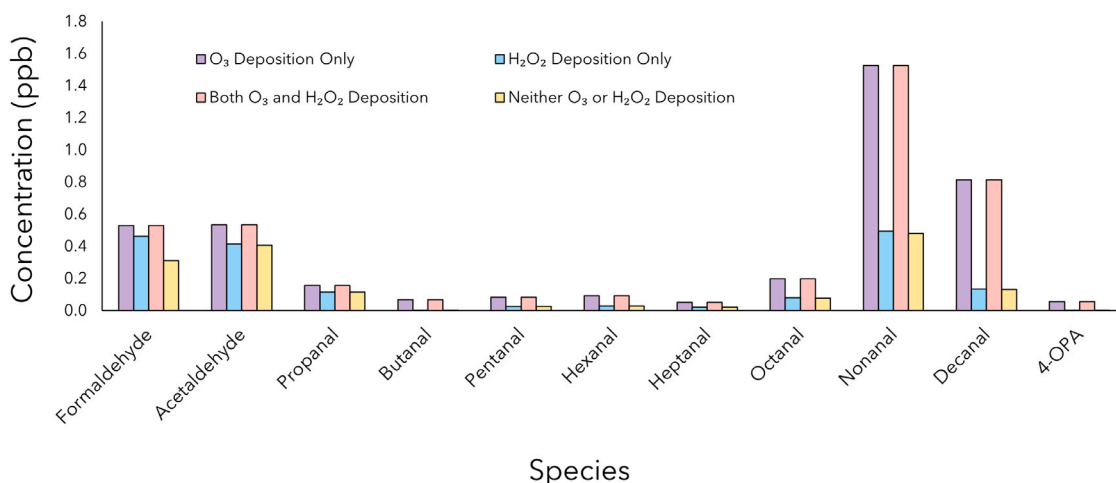
Fig. 5. The concentrations of straight-chained aldehyde species and 4-oxopentanal (4-OPA) in an office with and without oxidant deposition onto surfaces.

Uchiyama et al. (2015) reported concentrations of 0.16 ppb, 0.25 ppb, 1.4 ppb and 0.40 ppb for heptanal, octanal, nonanal and decanal respectively in Japanese homes. Our results (see Table 1) are comparable to these measured values, although our heptanal concentrations are slightly lower than measured. Indoor formaldehyde (19.2 ppb) and acetaldehyde (10.8 ppb) measurements from Uchiyama et al. (2015) however, were much higher than our results (factor of > 24 and > 11 higher respectively), although these are more likely to be influenced by human activities (such as cooking and cleaning) that we do not consider here. We acknowledge that, by ignoring these primary emissions for this study, our formaldehyde exposure levels are underestimated. These measurement studies have been carried out in various homes, each containing different materials and hence surface properties.

3.2. Secondary pollutants from surface interactions

Following oxidant deposition onto indoor surfaces in an occupied office, there was an increase in secondary pollutants, particularly in straight-chained aldehyde species compared to simulations with no deposition (Fig. 5). Following ozone deposition (for an average ozone concentration of 1.16 ppb), nonanal had the highest concentration (1.52 ppb), where emissions from plastic surfaces contributed the most. The concentration of decanal increased by $\approx 500\%$ following ozone deposition onto all available surfaces. However, the percentage change in most aldehyde concentrations following hydrogen peroxide deposition (for an average hydrogen peroxide concentration of 0.06 ppb) was small ($\approx 2\%$) and some concentrations even decreased slightly ($\approx -1\%$ change from the baseline).

Surface deposition gives rise to numerous secondary pollutants, some of which are harmful to health. Carslaw and Shaw (2019) defined a metric for comparing the potential health impacts of the secondary pollutants that arose under different indoor conditions, using the so-called 'Secondary Product Creation Potential (SPCP)'. This metric has been adapted to consider the different model simulations here and is defined as:

$$SPCP_{mod} = \Sigma \left(\begin{array}{c} [Total\ Organic\ Nitrates] + [PANs] + [O_3] + \\ [Glyoxal] + [Formaldehyde] + [Acetaldehyde] + \\ [Propanal] + [Butanal] + [Pentanal] + [Hexanal] + \\ [Heptanal] + [Octanal] + [Nonanal] + [Decanal] \end{array} \right)$$

(6)

$SPCP_{mod}$ therefore provides the sum of the concentrations of potentially harmful pollutants that are formed under different model scenarios with units of ppb. This metric is a guideline value only, as we currently lack information on the health effects of some of these species and they are unlikely to exert an equal influence on human health. However, it does provide a guide to the harmful concentrations that could be attained indoors under different conditions.

For the three modelled rooms (with both ozone and hydrogen peroxide deposition included), the $SPCP_{mod}$ values were 5.8, 6.7 and 4.8 ppb for the bedroom, kitchen and the office respectively, averaged over a full day. The concentrations of hexanal, octanal and nonanal were found to be highest in the bedroom (0.12 ppb, 0.19 ppb and 1.72 ppb), whereas the concentration of decanal was found to be highest in the office (0.77 ppb). There were assumed to be three people present in the office, giving skin a higher surface to volume ratio (Weschler et al., 2007) than the other rooms, resulting in a higher decanal concentration. The rest of the species present in Eq. (6) were found to have the highest concentrations in the kitchen.

3.3. Monitoring individual exposure to indoor air pollution

Using our results, we have considered a typical day spent indoors, to determine the exposure to specific indoor air pollutants that might be experienced (Fig. 6). We assumed that, on a typical day, a person will spend from: 00:00–07:00 h in the bedroom, 07:00–08:00 h in the kitchen, 08:00–08:30 h outdoors (walking to the office), 08:30–12:00 h in the office, 12:00–13:00 h outdoors (lunch break outside), 13:00–17:00 h in the office, 17:00–17:30 h walking home outdoors, 17:30–19:00 h in the kitchen, 19:00–22:00 h in the living room, then the rest of the day in the bedroom. It was assumed there were no high concentration activities such as cooking and cleaning. We assumed that the bedroom was a proxy for the living area given we did not study this particular micro-environment, but it is likely to be dominated by similar soft furnishings.

The concentrations of key indoor radical species varied throughout the day, depending on time and location. The highest concentrations for pollutants tend to correspond with time spent outdoors, given that many of them are predominantly generated outdoors under our simulated conditions (no cooking or cleaning). The highest indoor concentration of OH was 1.1×10^6 molecule cm^{-3} at 7:58 am in the kitchen. The OH concentration is driven by the reaction of NO with HO_2. NO concentrations are higher in the morning as it is generated by rush-hour traffic from outdoors, which will ingress inside.

Our results show that of our total pollutant exposure over the course of the day, 60% of OH, 81% of HO_2, 32% of O_3 and 77% of NO_x happens indoors. Our highest exposure to OH (32%) and NO_x (43%) is found in the office. Whereas, our highest exposure to HO_2 (53%) is found in the bedroom and living room, primarily due to the duration of time spent in these rooms over the course of a day. The total pollutant exposure (%) experienced in each micro-environment over the course of the day is given in Table S8.
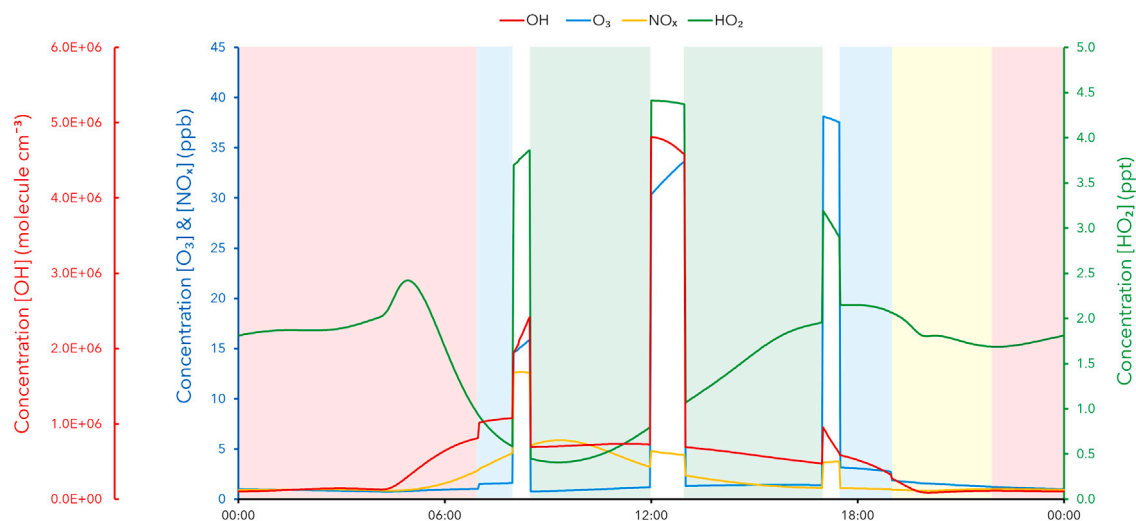
Fig. 6. The concentrations of OH (molecule cm^{-3}), HO$_2$ (ppt), O$_3$ and NO$_x$ (ppb) a person may be exposed to throughout the course of a typical day. The red shading on the graph indicates time spent in the bedroom, blue indicates time spent in the kitchen, green indicates time spent in the office, white indicates time spent outdoors and yellow indicates time spent in the living room.

3.4. Surfaces for the future

The INCHEM-Py model has been used to explore whether replacing individual surfaces can improve the indoor air quality. This is important as we consider more eco-friendly and sustainable materials to replace older, less environmentally beneficial surfaces in the future. In the past, we selected environmentally friendly materials based on the primary emission to indoor environments. This work shows that we need to consider the combination of the primary emissions and secondary chemistry to evaluate the impact of material interactions on indoor air quality. Thus, understanding total emissions from all new materials will help to inform decisions about which are best to use in different indoor environments.

We note that, in our study, in the bedroom and kitchen, wooden surfaces drive emission rates of shorter-chained aldehyde species (C$_1$-C$_5$) following oxidant deposition, compared to the other surfaces which were present. Whereas, we found that soft fabric and plastic surfaces account for the increase in longer-chained aldehyde species (C$_6$-C$_{10}$). Concrete surfaces had the lowest rate of production for the majority of the straight-chain aldehydes, primarily due its low surface-to-volume ratio. We also found that occupied rooms yielded an increase in the concentration of decanal and 4-oxopentanal (4-OPA), which are notably products of skin lipid ozonolysis (Weschler, 2016).

We ran model simulations, replacing wooden surfaces in the bedroom and the kitchen with concrete surfaces to determine the impact on indoor air chemistry. In addition, the plastic surfaces in the office were replaced with concrete surfaces. The percentage difference of the concentration of straight-chained aldehydes and key indoor species were then calculated.

When wooden materials are replaced by concrete equivalents in the bedroom and the kitchen respectively, most concentrations decreased: formaldehyde (by −14% and −24%), acetaldehyde (−19% and −28%), propanal (−30% and −45%), butanal (−76% and −81%), pentanal (−45% and −59%) and hexanal (−22% and −46%). Heptanal, octanal, nonanal and decanal concentrations all increased, but by minimal amounts (≈1%). This material replacement produced little change in radical concentrations in the bedroom and the kitchen.

In the office, where plastic was replaced by concrete, the concentration of short-chained aldehydes formaldehyde and propanal increased by 6% and 28% respectively, whereas octanal and decanal concentrations decreased by 19% and 10% respectively. However, the concentrations of HO$_2$ and RO$_2$ both increased by ≈37%, indicating a wider perturbation to the indoor chemistry. The concentration of

ozone nearly doubled under these conditions, owing to the lower ozone deposition velocity of concrete, therefore, ozone will have a higher ambient indoor concentration if plastic is replaced by concrete.

4. Conclusions

This study was undertaken to evaluate how indoor surfaces react with oxidants to impact indoor air quality in a kitchen and bedroom in a home environment and an office in a work environment. The model results demonstrated that the importance of individual surfaces varied between different rooms. The dominant surfaces often had a large product of deposition rate and surface area. Large unreactive surfaces and small reactive surfaces had minimal impact on modelled concentrations. Further experiments focussing on surface deposition of a wider range of oxidants and the respective production yields for emitted species and for a range of surfaces, would be highly beneficial.

This study has evaluated the exposure of indoor air pollution for a person over the course of a day and the respective health implications. It was determined that whilst indoors, OH concentration during the day was highest in the kitchen, whereas the HO$_2$ concentration was highest early in the morning, in the bedroom. A modified value of the Secondary Product Creation Potential (SPCP$_{mod}$) was highest in the kitchen and lowest in the office, indicating greater total exposure to potentially harmful air pollutants in the kitchen than the bedroom and the office. However, in order to make these assessments more accurate, we need more detailed information on the relative health impacts of the different species we have studied. This would help us to better understand how changing surfaces impact on health, as changing a surface will inevitably increase some concentrations, but reduce others.

CRediT authorship contribution statement

Toby J. Carter: Methodology, Software, Validation, Formal analysis, Investigation, Data curation, Writing – original draft, Visualization. **Dustin G. Poppendieck:** Provision of experimental data (hydrogen peroxide deposition velocities and surface emissions), Writing – review & editing. **David Shaw:** Methodology, Software, Resources, Data curation, Writing – review & editing. **Nicola Carslaw:** Conceptualization, Methodology, Software, Validation, Writing – original draft, Writing – review & editing, Supervision, Project administration, Funding acquisition.

Declaration of competing interest

The authors declare that they have no known competing financial interests or personal relationships that could have appeared to influence the work reported in this paper.

Data availability

Data from this project is available at https://doi.org/10.15124/f62de417-f8e8-4696-823c-fcbddecf150c, an online data repository hosted by the University of York (Carter et al., 2023).

Acknowledgements

Appendix A. Supplementary data

Supplementary material related to this article can be found online at https://doi.org/10.1016/j.atmosenv.2023.119598.

References

Abbass, O.A., Sailor, D.J., Gall, E.T., 2017. Effect of fiber material on ozone removal and carbonyl production from carpets. Atmos. Environ. 148, 42–48. http://dx.doi.org/10.1016/j.atmosenv.2016.10.034.

Ault, A.P., Grassian, V.H., Carslaw, N., Collins, D.B., Destaillats, H., Donaldson, D.J., Farmer, D.K., Jimenez, J.L., McNeill, V.F., Morrison, G.C., O'Brien, R.E., Shiraiwa, M., Vance, M.E., Wells, J., Xiong, W., 2020. Indoor surface chemistry: Developing a molecular picture of reactions on indoor interfaces. Chem 6 (12), 3203–3218. http://dx.doi.org/10.1016/j.chempr.2020.08.023, 10.1016/j.chempr.2020.08.023 https://linkinghub.elsevier.com/retrieve/pii/S2451929420304332.

Bari, M.A., Kindzierski, W.B., 2018. Ambient volatile organic compounds (VOCs) in Calgary, Alberta: Sources and screening health risk assessment. Sci. Total Environ. 631–632, 627–640. http://dx.doi.org/10.1016/j.scitotenv.2018.03.023.

Bari, M.A., Kindzierski, W.B., Spink, D., 2016. Twelve-year trends in ambient concentrations of volatile organic compounds in a community of the Alberta Oil Sands Region, Canada. Environ. Int. 91, 40–50. http://dx.doi.org/10.1016/j.envint.2016.02.015.

Baudic, A., Gros, V., Sauvage, S., Locoge, N., Sanchez, O., Sarda-Estève, R., Kalogridis, C., Petit, J.E., Bonnaire, N., Baisnée, D., Favez, O., Albinet, A., Sciare, J., Bonsang, B., 2016. Seasonal variability and source apportionment of volatile organic compounds (VOCs) in the Paris megacity (France). Atmos. Chem. Phys. 16 (18), 11961–11989. http://dx.doi.org/10.5194/acp-16-11961-2016.

Bekö, G., Weschler, C.J., Wierzbicka, A., Karottki, D.G., Toftum, J., Loft, S., Clausen, G., 2013. Ultrafine particles: Exposure and source apportionment in 56 Danish homes. Environ. Sci. Technol. 47 (18), 10240–10248. http://dx.doi.org/10.1021/es402429h.

Bloss, C., Wagner, V., Jenkin, M.E., Volkamer, R., Bloss, W.J., Lee, J.D., Heard, D.E., Wirtz, K., Martin-Reviejo, M., Rea, G., Wenger, J.C., Pilling, M.J., 2005. Development of a detailed chemical mechanism (MCMv3.1) for the atmospheric oxidation of aromatic hydrocarbons. Atmos. Chem. Phys. 5 (3), 641–664. http://dx.doi.org/10.5194/acp-5-641-2005.

Brickus, L.S., Cardoso, J.N., De Aquino Neto, F.R., 1998. Distributions of indoor and outdoor air pollutants in Rio de Janeiro, Brazil: Implications to indoor air quality in bayside offices. Environ. Sci. Technol. 32 (22), 3485–3490. http://dx.doi.org/10.1021/es980336x.

Cano-Ruiz, J., Kong, D., Balas, R., Nazaroff, W.W., 1993. Removal of reactive gases at indoor surfaces: Combining mass transport and surface kinetics. Atmos. Environ. Part A. General Top. 27 (13), 2039–2050. http://dx.doi.org/10.1016/0960-1686(93)90276-5.

Carslaw, N., 2007. A new detailed chemical model for indoor air pollution. Atmos. Environ. 41 (6), 1164–1179. http://dx.doi.org/10.1016/j.atmosenv.2006.09.038.

Carslaw, N., Fletcher, L., Heard, D., Ingham, T., Walker, H., 2017. Significant OH production under surface cleaning and air cleaning conditions: Impact on indoor air quality. Indoor Air 27 (6), 1091–1100. http://dx.doi.org/10.1111/ina.12394.

Carslaw, N., Mota, T., Jenkin, M.E., Barley, M.H., McFiggans, G., 2012. A significant role for nitrate and peroxide groups on indoor secondary organic aerosol. Environ. Sci. Technol. 46 (17), 9290–9298. http://dx.doi.org/10.1021/es301350x.

Carslaw, N., Shaw, D., 2019. Secondary product creation potential (SPCP): A metric for assessing the potential impact of indoor air pollution on human health. Environ. Sci. Process. Impacts 21 (8), 1313–1322. http://dx.doi.org/10.1039/c9em00140a.

Carslaw, N., Shaw, D., 2022. Modification of cleaning product formulations could improve indoor air quality. Indoor Air 32 (3), 1–13. http://dx.doi.org/10.1111/ina.13021.

Carter, T.J., Poppendieck, D.G., Shaw, D., Carslaw, N., 2023. Dataset for a modelling study of indoor air chemistry: The surface interactions of Ozone and hydrogen peroxide. http://dx.doi.org/10.15124/f62de417-f8e8-4696-823c-fcbddecf150c.

Cheng, Y.H., Lin, C.C., Hsu, S.C., 2015. Comparison of conventional and green building materials in respect of VOC emissions and ozone impact on secondary carbonyl emissions. Build. Environ. 87, 274–282. http://dx.doi.org/10.1016/j.buildenv.2014.12.025.

Chin, K., Laguerre, A., Ramasubramanian, P., Pleshakov, D., Stephens, B., Gall, E.T., 2019. Emerging investigator series: Primary emissions, ozone reactivity, and byproduct emissions from building insulation materials. Environ. Sci. Process. Impacts 21 (8), 1255–1267. http://dx.doi.org/10.1039/c9em00024k.

Clifford, G.M., Wenger, J.C., 2006. Rate coefficients for the gas-phase reaction of hydroxyl radicals with the dimethylbenzaldehydes. Int. J. Chem. Kinet. 38 (9), 563–569. http://dx.doi.org/10.1002/kin.20189.

Coleman, B.K., Destaillats, H., Hodgson, A.T., Nazaroff, W.W., 2008. Ozone consumption and volatile byproduct formation from surface reactions with aircraft cabin materials and clothing fabrics. Atmos. Environ. 42 (4), 642–654. http://dx.doi.org/10.1016/j.atmosenv.2007.10.001.

Cox, R.A., Penkett, S.A., 1972. Effect of relative humidity on the disappearance of ozone and sulphur dioxide in contained systems. Atmos. Environ. (1967) 6 (5), 365–368. http://dx.doi.org/10.1016/0004-6981(72)90203-X.

Cros, C.J., Morrison, G.C., Siegel, J.A., Corsi, R.L., 2012. Long-term performance of passive materials for removal of ozone from indoor air. Indoor Air 22 (1), 43–53. http://dx.doi.org/10.1111/j.1600-0668.2011.00734.x.

Destaillats, H., Maddalena, R.L., Singer, B.C., Hodgson, A.T., McKone, T.E., 2008. Indoor pollutants emitted by office equipment: A review of reported data and information needs. Atmos. Environ. 42 (7), 1371–1388. http://dx.doi.org/10.1016/j.atmosenv.2007.10.080.

Di, Y., Mo, J., Zhang, Y., Deng, J., 2017. Ozone deposition velocities on cotton clothing surface determined by the field and laboratory emission cell. Indoor Built Environ. 26 (5), 631–641. http://dx.doi.org/10.1177/1420326X16628315.

Dlugokencky, E., 2022. NOAA/GML CH4 trends. URL https://gml.noaa.gov/webdata/ccgg/trends/ch4/ch4_mm_gl.txt (Date Accessed: March 2022).

EEA, 2018. European Air Quality Portal. European Environment Agency, URL https://eeadmz1-cws-wp-air02.azurewebsites.net/ (Date Accessed: December 2021).

Fadeyi, M.O., Weschler, C.J., Tham, K.W., Wu, W.Y., Sultan, Z.M., 2013. Impact of human presence on secondary organic aerosols derived from ozone-initiated chemistry in a simulated office environment. Environ. Sci. Technol. 47 (8), 3933–3941. http://dx.doi.org/10.1021/es3050828.

Fischer, A., Ljungström, E., Langer, S., 2013. Ozone removal by occupants in a classroom. Atmos. Environ. 81, 11–17. http://dx.doi.org/10.1016/j.atmosenv.2013.08.054.

Gall, E., Darling, E., Siegel, J.A., Morrison, G.C., Corsi, R.L., 2013. Evaluation of three common green building materials for ozone removal, and primary and secondary emissions of aldehydes. Atmos. Environ. 77, 910–918. http://dx.doi.org/10.1016/j.atmosenv.2013.06.014.

Gallego, E., Roca, F.J., Perales, J.F., Guardino, X., Gadea, E., Garrote, P., 2016. Impact of formaldehyde and VOCs from waste treatment plants upon the ambient air nearby an urban area (Spain). Sci. Total Environ. 568, 369–380. http://dx.doi.org/10.1016/j.scitotenv.2016.06.007.

Gao, T., Andino, J.M., Rivera, C.C., Márquez, M.F., 2009. Rate constants of the gas-phase reactions of OH radicals with trans -2-hexenal, trans -2-octenal, and trans -2-nonenal. Int. J. Chem. Kinet. 41 (7), 483–489. http://dx.doi.org/10.1002/kin.20424.

Gaona Colmán, E., Blanco, M.B., Barnes, I., Wiesen, P., Teruel, M.A., 2017. Mechanism and product distribution of the O3-initiated degradation of (E)-2-Heptenal, (E)-2-Octenal, and (E)-2-nonenal. J. Phys. Chem. A 121 (27), 5147–5155. http://dx.doi.org/10.1021/acs.jpca.7b01857.

Grøntoft, T., 2002. Dry deposition of ozone on building materials. Chamber measurements and modelling of the time-dependent deposition. Atmos. Environ. 36 (36–37), 5661–5670. http://dx.doi.org/10.1016/S1352-2310(02)00701-X.

Grøntoft, T., Raychaudhuri, M.R., 2004. Compilation of tables of surface deposition velocities for O3, NO2 and SO2 to a range of indoor surfaces. Atmos. Environ. 38 (4), 533–544. http://dx.doi.org/10.1016/j.atmosenv.2003.10.010.

Hakola, H., Hellén, H., Tarvainen, V., Bäck, J., Patokoski, J., Rinne, J., 2009. Annual variations of atmospheric VOC concentrations in a boreal forest. Boreal Environ. Res. 14 (4), 722–730.

He, S.Z., Chen, Z.M., Zhang, X., Zhao, Y., Huang, D.M., Zhao, J.N., Zhu, T., Hu, M., Zeng, L.M., 2010. Measurement of atmospheric hydrogen peroxide and organic peroxides in Beijing before and during the 2008 Olympic games: Chemical and physical factors influencing their concentrations. J. Geophys. Res. 115 (D17), D17307. http://dx.doi.org/10.1029/2009JD013544.

Hellén, H., Praplan, A.P., Tykkä, T., Ylivinkka, I., Vakkari, V., Bäck, J., Petäjä, T., Kulmala, M., Hakola, H., 2018. Long-term measurements of volatile organic compounds highlight the importance of sesquiterpenes for the atmospheric chemistry of a boreal forest. Atmos. Chem. Phys. 18 (19), 13839–13863. http://dx.doi.org/10.5194/acp-18-13839-2018.

Hodgson, A.T., Ming, K.Y., Singer, B.C., 2004. Quantifying Object and Material Surface Areas in Residences. Lawrence Berkeley National Laboratory, pp. LBNL–56786.

Hodgson, A.T., Wooley, J.D., Daisey, J.M., 1993. Emissions of volatile organic compounds from new carpets measured in a large-scale environmental chamber. Air Waste 43 (3), 316–324. http://dx.doi.org/10.1080/1073161X.1993.10467136.

Jenkin, M.E., Saunders, S.M., Pilling, M.J., 1997. The tropospheric degradation of volatile organic compounds: A protocol for mechanism development. Atmos. Environ. 31 (1), 81–104. http://dx.doi.org/10.1016/S1352-2310(96)00105-7.

Jenkin, M.E., Saunders, S.M., Wagner, V., Pilling, M.J., 2003. Protocol for the development of the master chemical mechanism, MCM v3 (Part B): Tropospheric degradation of aromatic volatile organic compounds. Atmos. Chem. Phys. 3 (1), 181–193. http://dx.doi.org/10.5194/acp-3-181-2003.

Jenkin, M.E., Valorso, R., Aumont, B., Newland, M.J., Rickard, A.R., 2020. Estimation of rate coefficients for the reactions of O3 with unsaturated organic compounds for use in automated mechanism construction. Atmos. Chem. Phys. 20 (21), 12921–12937. http://dx.doi.org/10.5194/acp-20-12921-2020.

Jenkin, M.E., Valorso, R., Aumont, B., Rickard, A.R., 2019. Estimation of rate coefficients and branching ratios for reactions of organic peroxy radicals for use in automated mechanism construction. Atmos. Chem. Phys. 19 (11), 7691–7717. http://dx.doi.org/10.5194/acp-19-7691-2019.

Jenkin, M.E., Valorso, R., Aumont, B., Rickard, A.R., Wallington, T.J., 2018. Estimation of rate coefficients and branching ratios for gas-phase reactions of OH with aromatic organic compounds for use in automated mechanism construction. Atmos. Chem. Phys. 18 (13), 9329–9349. http://dx.doi.org/10.5194/acp-18-9329-2018.

Jenkin, M.E., Wyche, K.P., Evans, C.J., Carr, T., Monks, P.S., Alfarra, M.R., Barley, M.H., McFiggans, G.B., Young, J.C., Rickard, A.R., 2012. Development and chamber evaluation of the MCM v3.2 degradation scheme for β-caryophyllene. Atmos. Chem. Phys. 12 (11), 5275–5308. http://dx.doi.org/10.5194/acp-12-5275-2012.

Jenkin, M.E., Young, J.C., Rickard, A.R., 2015. The MCM v3.3.1 degradation scheme for isoprene. Atmos. Chem. Phys. 15 (20), 11433–11459. http://dx.doi.org/10.5194/acp-15-11433-2015.

Kahan, T.F., Washenfelder, R.A., Vaida, V., Brown, S.S., 2012. Cavity-enhanced measurements of hydrogen peroxide absorption cross sections from 353 to 410 nm. J. Phys. Chem. A 116 (24), 5941–5947. http://dx.doi.org/10.1021/jp2104616.

Kang, K., Kim, H., Kim, D.D., Lee, Y.G., Kim, T., 2019. Characteristics of cooking-generated PM 10 and PM 2.5 in residential buildings with different cooking and ventilation types. Sci. Total Environ. 668, 56–66. http://dx.doi.org/10.1016/j.scitotenv.2019.02.316.

Katsoyiannis, A., Leva, P., Kotzias, D., 2008. VOC and carbonyl emissions from carpets: A comparative study using four types of environmental chambers. J. Hard Mater. 152 (2), 669–676. http://dx.doi.org/10.1016/j.jhazmat.2007.07.058.

Kerdouci, J., Picquet-Varrault, B., Durand-Jolibois, R., Gaimoz, C., Doussin, J.F., 2012. An experimental study of the gas-phase reactions of no3 radicals with a series of unsaturated aldehydes: Trans -2-hexenal, trans -2-heptenal, and trans -2-octenal. J. Phys. Chem. A 116 (41), 10135–10142. http://dx.doi.org/10.1021/jp3071234.

Klenø, J.G., Clausen, P.A., Weschler, C.J., Wolkoff, P., 2001. Determination of ozone removal rates by selected building products using the FLEC emission cell. Environ. Sci. Technol. 35 (12), 2548–2553. http://dx.doi.org/10.1021/es000284n.

Klepeis, N.E., Nelson, W.C., Ott, W.R., Robinson, J.P., Tsang, A.M., Switzer, P., Behar, J.V., Hern, S.C., Engelmann, W.H., 2001. The national human activity pattern survey (NHAPS): A resource for assessing exposure to environmental pollutants. J. Exposure Anal. Environ. Epidemiol. 11 (3), 231–252. http://dx.doi.org/10.1038/sj.jea.7500165.

Kruza, M., Carslaw, N., 2019. How do breath and skin emissions impact indoor air chemistry? Indoor Air 29 (3), 369–379. http://dx.doi.org/10.1111/ina.12539.

Kruza, M., Lewis, A.C., Morrison, G.C., Carslaw, N., 2017. Impact of surface ozone interactions on indoor air chemistry: A modeling study. Indoor Air 27 (5), 1001–1011. http://dx.doi.org/10.1111/ina.12381.

Kruza, M., McFiggans, G., Waring, M.S., Wells, J.R., Carslaw, N., 2020. Indoor secondary organic aerosols: Towards an improved representation of their formation and composition in models. Atmos. Environ. 240 (August), 117784. http://dx.doi.org/10.1016/j.atmosenv.2020.117784.

Lakey, P.S., Wisthaler, A., Berkemeier, T., Mikoviny, T., Pöschl, U., Shiraiwa, M., 2017. Chemical kinetics of multiphase reactions between ozone and human skin lipids: Implications for indoor air quality and health effects. Indoor Air 27 (4), 816–828. http://dx.doi.org/10.1111/ina.12360.

Lamble, S.P., Corsi, R.L., Morrison, G.C., 2011. Ozone deposition velocities, reaction probabilities and product yields for green building materials. Atmos. Environ. 45 (38), 6965–6972. http://dx.doi.org/10.1016/j.atmosenv.2011.09.025.

Lin, C.C., Hsu, S.C., 2015. Deposition velocities and impact of physical properties on ozone removal for building materials. Atmos. Environ. 101, 194–199. http://dx.doi.org/10.1016/j.atmosenv.2014.11.029.

Liu, Y., Misztal, P.K., Arata, C., Weschler, C.J., Nazaroff, W.W., Goldstein, A.H., 2021. Observing ozone chemistry in an occupied residence. Proc. Natl. Acad. Sci. 118 (6), e2018140118. http://dx.doi.org/10.1073/pnas.2018140118.

Liu, L., Wang, X., Chen, J., Xue, L., Wang, W., Wen, L., Li, D., Chen, T., 2018. Understanding unusually high levels of peroxyacetyl nitrate (PAN) in winter in Urban Jinan, China. J. Environ. Sci. (China) 71, 249–260. http://dx.doi.org/10.1016/j.jes.2018.05.015.

Lü, H., Wen, S., Feng, Y., Wang, X., Bi, X., Sheng, G., Fu, J., 2006. Indoor and outdoor carbonyl compounds and BTEX in the hospitals of Guangzhou, China. Sci. Total Environ. 368 (2–3), 574–584. http://dx.doi.org/10.1016/j.scitotenv.2006.03.044.

Manuja, A., Ritchie, J., Buch, K., Wu, Y., Eichler, C.M., Little, J.C., Marr, L.C., 2019. Total surface area in indoor environments. Environ. Sci. Process. Impacts 21 (8), 1384–1392. http://dx.doi.org/10.1039/c9em00157c.

Mentese, S., Bas, B., 2020. A year-round motoring of ambient volatile organic compounds across Dardanelles strait. J. Chem. Metrol. 14 (2), 177–189. http://dx.doi.org/10.25135/jcm.51.20.09.1816.

Ministry of Housing, Communities & Local Government (UK Government), 2019. Ventilation and Indoor Air Quality in New Homes . Ministry of Housing, Communities and Local Government (United Kingdom), pp. 1–87, URL https://assets.publishing.service.gov.uk/government/uploads/system/uploads/attachment_data/file/835208/Research_-_ventilation_and_indoor_air_quality.pdf (Date Accessed: October 2021).

Morgan, M., Cruickshank, H., 2014. Quantifying the extent of space shortages: English dwellings. Buil. Res. Inform. 42 (6), 710–724. http://dx.doi.org/10.1080/09613218.2014.922271.

Morrison, G.C., Nazaroff, W.W., 2000. The rate of Ozone uptake on carpets: Experimental studies. Environ. Sci. Technol. 34 (23), 4963–4968. http://dx.doi.org/10.1021/es001361h.

Morrison, G.C., Nazaroff, W.W., 2002. Ozone interactions with carpet: Secondary emissions of aldehydes. Environ. Sci. Technol. 36 (10), 2185–2192. http://dx.doi.org/10.1021/es0113089.

Mueller, F.X., Loeb, L., Mapes, W.H., 1973. Decomposition rates of Ozone in living areas. Environ. Sci. Technol. 7 (4), 342–346. http://dx.doi.org/10.1021/es60076a003.

Nazaroff, W.W., 2021. Residential air-change rates: A critical review. Indoor Air 31 (2), 282–313. http://dx.doi.org/10.1111/ina.12785.

Nazaroff, W.W., Weschler, C.J., 2004. Cleaning products and air fresheners: Exposure to primary and secondary air pollutants. Atmos. Environ. 38 (18), 2841–2865. http://dx.doi.org/10.1016/j.atmosenv.2004.02.040.

Nicolas, M., Ramalho, O., Maupetit, F., 2007. Reactions between ozone and building products: Impact on primary and secondary emissions. Atmos. Environ. 41 (15), 3129–3138. http://dx.doi.org/10.1016/j.atmosenv.2006.06.062.

Nørgaard, A.W., Kudal, J.D., Kofoed-Sørensen, V., Koponen, I.K., Wolkoff, P., 2014. Ozone-initiated VOC and particle emissions from a cleaning agent and an air freshener: Risk assessment of acute airway effects. Environ. Int. 68, 209–218. http://dx.doi.org/10.1016/j.envint.2014.03.029.

Poppendieck, D., Hubbard, H., Corsi, R.L., 2021. Hydrogen peroxide vapor as an indoor disinfectant: Removal to indoor materials and associated emissions of organic compounds. Environ. Sci. Technol. Lett. 8 (4), 320–325. http://dx.doi.org/10.1021/acs.estlett.0c00948.

Poppendieck, D., Hubbard, H., Ward, M., Weschler, C., Corsi, R.L., 2007a. Ozone reactions with indoor materials during building disinfection. Atmos. Environ. 41 (15), 3166–3176. http://dx.doi.org/10.1016/j.atmosenv.2006.06.060.

Poppendieck, D.G., Hubbard, H.F., Weschler, C.J., Corsi, R.L., 2007b. Formation and emissions of carbonyls during and following gas-phase ozonation of indoor materials. Atmos. Environ. 41 (35), 7614–7626. http://dx.doi.org/10.1016/j.atmosenv.2007.05.049.

Rai, A.C., Guo, B., Lin, C.H., Zhang, J., Pei, J., Chen, Q., 2014. Ozone reaction with clothing and its initiated VOC emissions in an environmental chamber. Indoor Air 24 (1), 49–58. http://dx.doi.org/10.1111/ina.12058.

Reiss, R., Ryan, P.B., Koutrakis, P., 1994. Modeling Ozone deposition onto indoor residential surfaces. Environ. Sci. Technol. 28 (3), 504–513. http://dx.doi.org/10.1021/es00052a025.

Rim, D., Gall, E.T., Maddalena, R.L., Nazaroff, W.W., 2016. Ozone reaction with interior building materials: Influence of diurnal ozone variation, temperature and humidity. Atmos. Environ. 125, 15–23. http://dx.doi.org/10.1016/j.atmosenv.2015.10.093.

Ruiz-Jimenez, J., Heiskanen, I., Tanskanen, V., Hartonen, K., Riekkola, M.-L., 2022. Analysis of indoor air emissions: From building materials to biogenic and anthropogenic activities. J. Chromatogr. Open 2 (March), 100041. http://dx.doi.org/10.1016/j.jcoa.2022.100041.

Sabersky, R.H., Sinema, D.A., Shair, F.H., 1973. Concentrations, decay rates, and removal of Ozone and their relation to establishing clean indoor air. Environ. Sci. Technol. 7 (4), 347–353. http://dx.doi.org/10.1021/es60076a001.

Salthammer, T., 2019. Formaldehyde sources, formaldehyde concentrations and air exchange rates in European housings. Build. Environ. 150 (October 2018), 219–232. http://dx.doi.org/10.1016/j.buildenv.2018.12.042.

Saunders, S.M., Jenkin, M.E., Derwent, R.G., Pilling, M.J., 2003. Protocol for the development of the master chemical mechanism, MCM v3 (part A): Tropospheric degradation of non-aromatic volatile organic compounds. Atmos. Chem. Phys. 3 (1), 161–180. http://dx.doi.org/10.5194/acp-3-161-2003.

Schripp, T., Langer, S., Salthammer, T., 2012. Interaction of ozone with wooden building products, treated wood samples and exotic wood species. Atmos. Environ. 54, 365–372. http://dx.doi.org/10.1016/j.atmosenv.2012.02.064.

Shaw, D., Carslaw, N., 2021. INCHEM-Py: An open source Python box model for indoor air chemistry. J. Open Source Softw. 6 (63), 3224. http://dx.doi.org/10.21105/joss.03224.

Shen, J., Gao, Z., 2018. Ozone removal on building material surface: A literature review. Build. Environ. 134 (March), 205–217. http://dx.doi.org/10.1016/j.buildenv.2018.02.046.

Shin, S.H., Jo, W.K., 2013. Temporal characteristics of volatile organic compounds in newly-constructed residential buildings: Concentration and source. Environ. Eng. Res. 18 (3), 169–176. http://dx.doi.org/10.4491/eer.2013.18.3.169.

Simmons, A., Colbeck, I., 1990. Resistance of various building materials to ozone deposition. Environ. Technol. (United Kingdom) 11 (10), 973–978. http://dx.doi.org/10.1080/09593339009384949.

Sturaro, A., Rella, R., Parvoli, G., Ferrara, D., 2010. Long-term phenol, cresols and BTEX monitoring in urban air. Environ. Monit. Assess. 164 (1–4), 93–100. http://dx.doi.org/10.1007/s10661-009-0877-x.

Tamás, G., Weschler, C.J., Bakó-Biró, Z., Wyon, D.P., Strøm-Tejsen, P., 2006. Factors affecting ozone removal rates in a simulated aircraft cabin environment. Atmos. Environ. 40 (32), 6122–6133. http://dx.doi.org/10.1016/j.atmosenv.2006.05.034.

Uchiyama, S., Tomizawa, T., Tokoro, A., Aoki, M., Hishiki, M., Yamada, T., Tanaka, R., Sakamoto, H., Yoshida, T., Bekki, K., Inaba, Y., Nakagome, H., Kunugita, N., 2015. Gaseous chemical compounds in indoor and outdoor air of 602 houses throughout Japan in winter and summer. Environ. Res. 137, 364–372. http://dx.doi.org/10.1016/j.envres.2014.12.005.

Vichi, F., Mašková, L., Frattoni, M., Imperiali, A., Smolík, J., 2016. Simultaneous measurement of nitrous acid, nitric acid, and nitrogen dioxide by means of a novel multipollutant diffusive sampler in libraries and archives. Heritage Sci. 4 (1), 1–8. http://dx.doi.org/10.1186/s40494-016-0074-5.

Wang, N., Ernle, L., Bekö, G., Wargocki, P., Williams, J., 2022a. Emission rates of volatile organic compounds from humans. Environ. Sci. Technol. 56, 4838–4848. http://dx.doi.org/10.1021/acs.est.1c08764.

Wang, Z., Kowal, S.F., Carslaw, N., Kahan, T.F., 2020. Photolysis-driven indoor air chemistry following cleaning of hospital wards. Indoor Air 30 (6), 1241–1255. http://dx.doi.org/10.1111/ina.12702.

Wang, H., Morrison, G.C., 2006. Ozone-initiated secondary emission rates of aldehydes from indoor surfaces in four homes. Environ. Sci. Technol. 40 (17), 5263–5268. http://dx.doi.org/10.1021/es060080s.

Wang, H., Morrison, G., 2010. Ozone-surface reactions in five homes: Surface reaction probabilities, aldehyde yields, and trends. Indoor Air 20 (3), 224–234. http://dx.doi.org/10.1111/j.1600-0668.2010.00648.x.

Wang, Z., Shaw, D., Kahan, T., Schoemaecker, C., Carslaw, N., 2022b. A modeling study of the impact of photolysis on indoor air quality. Indoor Air 32 (6), http://dx.doi.org/10.1111/ina.13054.

Waring, M.S., Siegel, J.A., 2013. Indoor secondary organic aerosol formation initiated from reactions between Ozone and surface-sorbed d-Limonene. Environ. Sci. Technol. 47 (12), 6341–6348. http://dx.doi.org/10.1021/es400846d.

Waring, M.S., Wells, J.R., 2015. Volatile organic compound conversion by ozone, hydroxyl radicals, and nitrate radicals in residential indoor air: Magnitudes and impacts of oxidant sources. Atmos. Environ. 106 (3), 382–391. http://dx.doi.org/10.1016/j.atmosenv.2014.06.062.

Weschler, C.J., 2000. Ozone in indoor environments: Concentration and chemistry. Indoor Air 10 (4), 269–288. http://dx.doi.org/10.1034/j.1600-0668.2000.010004269.x.

Weschler, C.J., 2016. Roles of the human occupant in indoor chemistry. Indoor Air 26 (1), 6–24. http://dx.doi.org/10.1111/ina.12185.

Weschler, C.J., Wisthaler, A., Cowlin, S., Tamás, G., Strøm-Tejsen, P., Hodgson, A.T., Destaillats, H., Herrington, J., Zhang, J., Nazaroff, W.W., 2007. Ozone-initiated chemistry in an occupied simulated aircraft cabin. Environ. Sci. Technol. 41 (17), 6177–6184. http://dx.doi.org/10.1021/es0708520.

Wisthaler, A., Weschler, C.J., 2010. Reactions of ozone with human skin lipids: Sources of carbonyls, dicarbonyls, and hydroxycarbonyls in indoor air. Proc. Natl. Acad. Sci. USA 107 (15), 6568–6575. http://dx.doi.org/10.1073/pnas.0904498106.

Wong, J.P., Carslaw, N., Zhao, R., Zhou, S., Abbatt, J.P., 2017. Observations and impacts of bleach washing on indoor chlorine chemistry. Indoor Air 27 (6), 1082–1090. http://dx.doi.org/10.1111/ina.12402.

Xiong, J., Chen, F., Sun, L., Yu, X., Zhao, J., Hu, Y., Wang, Y., 2019. Characterization of VOC emissions from composite wood furniture: Parameter determination and simplified model. Build. Environ. 161 (April), 106237. http://dx.doi.org/10.1016/j.buildenv.2019.106237.

Xue, L.K., Saunders, S.M., Wang, T., Gao, R., Wang, X.F., Zhang, Q.Z., Wang, W.X., 2015. Development of a chlorine chemistry module for the master chemical mechanism. Geosci. Model Dev. 8 (10), 3151–3162. http://dx.doi.org/10.5194/gmd-8-3151-2015.

Yao, M., Ke, L., Liu, Y., Luo, Z., Zhao, B., 2020. Measurement of ozone deposition velocity onto human surfaces of Chinese residents and estimation of corresponding production of oxidation products. Environ. Pollut. 266, 115215. http://dx.doi.org/10.1016/j.envpol.2020.115215.

Ye, W., Wang, H., Chen, Z., Zhang, X., 2020. Ozone deposition on free-running indoor materials and the corresponding volatile organic compound emissions: Implications for ventilation requirements. Appl. Sci. 10 (12), 4146. http://dx.doi.org/10.3390/app10124146.

Zhou, S., Liu, Z., Wang, Z., Young, C.J., Vandenboer, T.C., Guo, B.B., Zhang, J., Carslaw, N., Kahan, T.F., 2020. Hydrogen peroxide emission and fate indoors during non-bleach cleaning: A chamber and modeling study. Environ. Sci. Technol. 54 (24), 15643–15651. http://dx.doi.org/10.1021/acs.est.0c04702.